metals

MDPI

Article

Advances in Thermochemical Synthesis and Characterization of the Prepared Copper/Alumina Nanocomposites

Marija Korać [1], Željko Kamberović [1], Zoran Anđić [2] and Srećko Stopić [3,*]

[1] Faculty of Technology and Metallurgy, Karnegijeva 4, 11120 Belgrade, Serbia; marijakorac@tmf.bg.ac.rs (M.K.); kamber@tmf.bg.ac.rs (Ž.K.)

[2] Innovation center of Faculty of Chemistry Ltd., University of Belgrade, 12-16 Studentski trg, 11000 Belgrade, Serbia; zoranandjic@yahoo.com

[3] IME Process Metallurgy and Metal Recycling, RWTH Aachen University, Intzestrasse 3, 52056 Aachen, Germany

* Correspondence: sstopic@ime-aachen.de; Tel.: +49-241-80-95-860

Received: 30 April 2020; Accepted: 26 May 2020; Published: 28 May 2020

Abstract: This paper presents thermochemical synthesis of copper/alumina nanocomposites in a Cu-Al_2O_3 system with 1–2.5 wt.% of alumina and their characterization, which included: transmission electron microscopy: focused ion beam (FIB), analytical electron microscopy (AEM) and high resolution transmission electron microscopy (HRTEM). Thermodynamic analysis was used to study the formation mechanism of desirable products during drying, thermal decomposition and reduction processes. Upon synthesis of powders, samples were cold pressed (2 GPa) in tools dimension 8 × 32 × 2 mm and sintered at temperatures within the range 800–1000 °C for 15 to 120 min in a hydrogen atmosphere. Results of characterization showed that dispersion-strengthened compacts could be produced by sintering of thermo-chemically prepared Cu-Al_2O_3 powders with properties suitable for material application, such as a contact material exhibiting high strength and high electrical conductivity at the same time. Additional research was carried out in order to analyze the application of the obtained nanocomposite powders for the synthesis of copper/alumina nanocomposites by a new method, which is a combination of a thermochemical procedure and mechanical alloying. The measured values of an electric conductivity and hardness were compared with ones in literature, confirming an advantage of the proposed combined strategy.

Keywords: synthesis; oxide; nanocomposites; characterization; copper; alumina; thermochemistry

1. Introduction

Research of metal matrix composite (MMC) materials has considerably intensified since its first mention in the 1950s [1]. Various combinations of base (Al, Cu, Ni, Mg, Ti, Fe, Co, etc.) and reinforcing material (e.g., oxides, borides, carbides, fibers, tubes) have been studied [2]. Through selection of appropriate combinations and ratios of materials, a wide spectrum of properties can be achieved, followed by extensive industrial applications.

Copper is considered the most significant base material for industrial applications, due to its good electrical and heat conductivity. Disadvantages of copper are its mechanical properties, such as high ductility, low wear resistance and thermodynamic instability at elevated temperatures. One of the possibilities for overcoming poor mechanical properties is reinforcement by dispersion strengthening; i.e., the introduction of fine ceramic particles. By the dispersion strengthening of copper, significant increases in mechanical properties can be achieved, with low adverse impacts on

its electrical and heat conductivity. The main requirements for dispersed particles are higher thermodynamic stability at elevated temperatures; higher hardness, strength and wear resistance; and low solubility in base metal. Appropriate size and even distribution of dispersed particles also contribute to a positive effect via dispersion strengthening [3]. Finer particles with homogenous distribution and low volume fraction of dispersed particles in the total volume of the base metal will act as obstacles to dislocation motion, even at elevated temperatures without significant effects on conductivities, both thermal and electrical [4–7].

One of the most widely used oxides is alumina, which fulfills all the requirements for the dispersed particles and has low cost at the same time [8]. Additionally, alumina can increase the temperature of recrystallization of the copper matrix and demonstrates excellent strength at elevated temperature by pinning grain and sub-grain boundaries of the matrix. Finally, alumina particles add to strengthening by blocking the movement of dislocations [7,9,10]. The usual amount of alumina used for dispersion strengthening is 0.5–5.0 wt.% [11], but significant results regarding particle size can be achieved even with higher amounts, such as 50 wt.% of Al_2O_3 [12].

There are numerous routes for the synthesis of metal–matrix composites, but nowadays two main routes are the mechanical alloying and thermochemical route. Mechanical alloying is extensively used method for synthesizing of nanocrystalline materials by severe plastic deformation on the powder using high-energy ball milling technique [13–16]. This technique commonly employed for the prevention of formation of clusters and agglomerates enables the production of uniformly dispersed fine particles in a metal–matrix. On the other hand, using the thermochemical method [17] where input materials are in a liquid state enables production of finer particles and much more homogeneous structure of the final powder, which further contributes to the increase in the mechanical properties for the final product through various strengthening mechanisms.

Authors have also developed a new synthesis route based on the combination of routes mentioned above [18]. This route may be regarded as a new strategy for materials in the Cu-Al_2O_3 system, even though some phases of this process have been previously investigated by the authors [19–21]. Additionally, previous attempts have been made by authors for application of similar process in the system Cu-Ag-Al_2O_3, where a three-component system was produced by mechanically alloying the thermo-chemically-synthesized Cu-Al_2O_3 and Cu-Ag powder [22].

The main aim of this work was to investigate a thermochemical synthesis of metallic particles and nanocomposite with a microstructure and strengthening mechanism of copper with finely dispersed alumina particles. A novelty of this synthesis is a decreased reduction temperature for chemical reaction of the powder in a hydrogen atmosphere at 350 °C, which is an advantage in contrast to 820 °C for 1 h to produce the final Cu–Al_2O_3 nanocomposite powder, as described by Seyedraoufi et al. [23]. It can be very important point for decreasing production costs. A thermodynamic analysis of the reduction, spray drying and synthesis reactions was performed in order to predict a chemical behavior of the compounds. Amirjan et al. [24] have used artificial neural networks to predict Cu-Al_2O_3 properties. In order to prepare copper based composites, copper powder with four different amounts of Al_2O_3 reinforcement (1, 1.5, 2, 2.5 wt%) were mechanically alloyed, and the consolidated compacts of prepared powders were sintered in five different temperatures of 725–925 °C at seven several sintering times of 15–180 min. Guevara et al [25] have studied the synthesis of copper-alumina composites by mechanical milling via an analysis of materials and manufacturing processes. Ha et al. [26] studied the fabrication of Al_2O_3 dispersion strengthened copper alloy by spray in-situ synthesis casting process above 1250 °C as a new method. Mohammadi, E. et al. [27] used a combustion method for the synthesis of Cu-Al_2O_3, which take place in a short time at temperatures higher than 1000 °C. Generally, our synthesis method offers a cost-friendly process for the synthesis of Cu-Al_2O_3 in comparison to other processes [27].

These powders could be used for production of sintered materials with properties suitable for material applications, such as contact material exhibiting high strength and high electrical conductivity at the same time.

Some comparative results for different synthesis methods are presented, indicating that by mechanical alloying of atomized copper powders with produced composites, followed by thermo-mechanical treatment, sintered materials with improved properties could be produced.

2. Experimental

Water soluble copper and aluminum nitrates, $Cu(NO_3)_2 \cdot 3H_2O$ and $Al(NO_3)_3 \cdot 9H_2O$, were used to synthesize a two-component nanocomposite Cu-Al_2O_3 powder by the thermochemical procedure.

The synthesis was carried out through four stages, as presented in Figure 1.

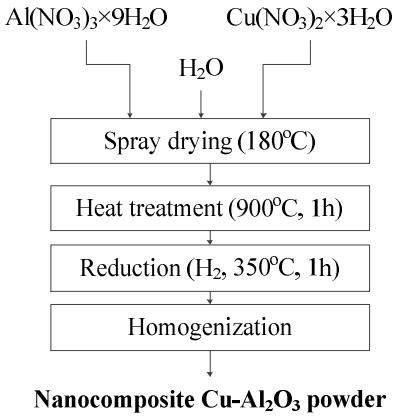

Figure 1. Flowsheet of the synthesis of Cu-Al_2O_3 nanocomposite powder by the thermochemical procedure [28].

Process temperatures are derived from thermodynamic consideration of the process and the following six chemical reactions:

Spray drying:

$$Cu(NO_3)_2 \cdot 6H_2O = Cu(NO_3)_2 + 6H_2O \quad (1)$$

$$Al(NO_3)_3 \cdot 6H_2O = Al(NO_3)_3 + 6H_2O \quad (2)$$

Heat treatment:

$$Cu(NO_3)_2 = CuO + N_2O_5 \quad (3)$$

$$2Al(NO_3)_3 = Al_2O_3 + 3\,N_2O_5 \quad (4)$$

Reduction:

$$CuO + H_2 = Cu + H_2O \quad (5)$$

$$Al_2O_3 + 3H_2 = 2Al + 3H_2O \quad (6)$$

Using HSC Chemistry® software package 6.12 (Outotec, Espoo, Finland), chemical and thermodynamic parameters of the processes for synthesis Cu-Al_2O_3 composites were analyzed. As shown at Figure 2, the calculated values of Gibbs energy of reactions versus temperature (up 1000 °C) for reactions (1)–(6) have positive and negative values; negative values confirmed the possibility for the beginning of these chemical reactions at the studied temperature. Because of the high positive values of Gibbs energy (more than 800 kJ/mol), reduction of aluminum oxide with hydrogen (as shown with Equation (6)) is not possible between 25 and 1000 °C.

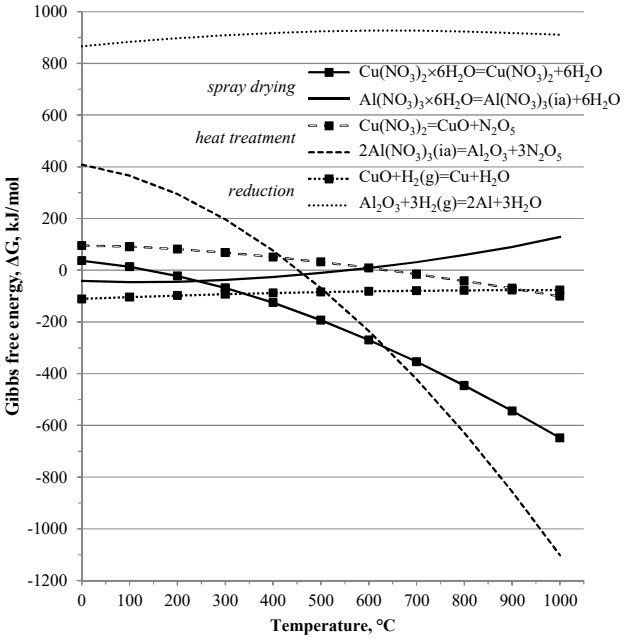

Figure 2. Gibbs energy of reactions versus temperature.

The first stage is the preparation of 50 wt.% aqueous solutions of $Cu(NO_3)_2 \cdot 3H_2O$ and $Al(NO_3)_3 \cdot 9H_2O$ (the quantities of salt were set so that the requested composition of a Cu-Al_2O_3 nanocomposite system with 5 wt.% of alumina could be produced). The second phase is spray drying of nitrate solution using Mini Spray Dryer B-290 Advance (BÜCHI Labortechnik GmbH, Essen, Germany) for producing the precursor powder, with inlet/outlet temperature 190/143 °C and a solution flow rate of 10% pump power. The third stage is oxidative calcination of the precursor powder in an air atmosphere at 900 °C for 1 h to form copper oxide and the phase transformation of Al_2O_3 up to the thermodynamically stable α-Al_2O_3 phase. Final fourth stage was the reduction of thermally treated powders in hydrogen atmosphere flow rate 20 L/h at 350 °C for one hour, where copper oxide was transformed into elementary copper, while Al_2O_3 remained unchanged.

All temperatures were below the temperatures the melting temperature of Cu (1085 °C) [29] and Al_2O_3 (2072 °C) [30].

In previous work of authors procedures [22,29] and process parameters [21,31] are fully described for the synthesis of two-component nanostructured composite materials.

The obtained powders were cold-pressed (force 500 kN, calculated pressure 2 GPa) in tools with dimensions of 8 × 32 × 2 mm and sintered at temperatures within 800–1000 °C for 15 to 120 min in a hydrogen atmosphere. Kinetics of the sintering process were determined and presented elsewhere [21].

Characterization of compacted powders after sintering at 900 °C for 2h included transmission electron microscopy: analytical electron microscopy (AEM), high resolution transmission electron microscopy (HRTEM) and focused ion beam (FIB) at e-beam 5.00 kV. The powder to be tested is suspended in a liquid (water, ethanol or butanol) with the aid of an ultrasonic device. Depending on particle size, requirements and type of examination, the powder is first ground. By means of a pipette a drop of suspension is taken up and placed on a carbon carrier net. The liquid is then allowed to evaporate (dry) under a lamp, resulting in a C-carrier net with the powder on top. After this powder preparation, our sample was studied by TEM Analysis. HRTEM analysis was performed using Philips CM200/FEG (FEI Company, Hillsboro, OR, USA).

Mechanical properties of sintered samples were also investigated and are presented in authors' previous research [28].

Ames Portable Hardness Tester was employed for hardness measurements using a 1/16" ball with an applied load of 60 kg. For electrical conductivity measurement, SIGMATEST 2.069

(FOERSTER, Pittsburgh, PA, USA) operating at 120 kHz and with an 8 mm electrode diameter was used.

Values of hardness and electrical conductivity represent the mean values of at least six measurements conducted on the same composite.

3. Results and Discussion

In previous work of the authors [22], the results of determination of fluidness, pouring density and specific area of the obtained nanostructured composites with different amounts of Al_2O_3 dispersed in the copper matrix showed that all the investigated powders are not fluid and that mean values of pouring density and specific area are the same for different contents of Al_2O_3 up to the 5% investigated.

Additionally, in some previous studies of the authors [21,22,32] the results of differential thermal and thermogravimetric analysis (DTA-TGA) and scanning electron microscopy can be found, which show the flow of phase transformations during the process of oxidation, and the morphologies of the obtained powders.

Only peaks corresponding to the nitrates of copper and aluminum were identified in the structure during XRD examination of the precursor powder produced by spray drying an aqueous solution of copper and aluminum nitrates, which is in accordance with the experiment set-up [20–22]. X-ray diffraction analysis after annealing of dried powder exhibited peaks corresponding to CuO and Al_2O_3, and one unidentified peak. According to Lee [33] this peak corresponds to a third phase, $Cu_xAl_yO_z$, which appears in the structure due to the eutectic reaction of (Cu + Cu_2O) with Al_2O_3.

The produced powders were analyzed by AEM with corresponding EDX, as shown in the previous works of authors [34]. Based on AEM analysis, particles 20–50 nm in size, are clearly noticeable, as is the presence of agglomerates >100 nm. Particles are irregularly shaped; there are nodular individual particles with rough surface morphology. EDS analysis of marked spot show that the identified peaks correspond to Cu, Al and O. The intensities of peaks correspond to demanded compositions of the examined systems; therefore, the peak corresponding to copper is considerably higher than the peaks corresponding to aluminum and oxygen.

In order to identify the third phase, the authors performed additional research through the synthesis of Cu-50 wt.% by a thermochemical procedure. X-ray diffraction analysis of the obtained sample, presented in [18], shows the presence of copper peaks and $CuAl_2O_4$ compounds, which may represent a metastable phase that developed in the microstructure during the process of powder synthesis, thermal treatment and reduction on the surface of the contact between Cu and Al_2O_3 and is a seed for the development of the third phase during the sintering process.

FIB analysis of the sintered Cu-Al_2O_3 system based on the powders obtained by the thermochemical procedure, as shown in Figure 3, is characteristic for the final stage of sintering. FIB analysis did not indicate even at considerably higher magnifications, the existence of a phase rich with alumina. The bright fields are identified, i.e., a phase rich with copper, and gray fields, which can lead to a possible existence of the third $Cu_xAl_yO_z$ phase identified by X-ray diffraction analysis [18]. The formation of this phase is thermodynamically possible on Cu-Al contact surfaces. During eutectic joining of copper and Al_2O_3, the eutecticum formed by heating up to the eutectic temperature expands and reacts with Al_2O_3 creating $Cu_xAl_yO_z$, which is compatible with both phases on the inter-surface. According to [35,36], the process of formation of the third phase is developed through the following reactions: $2CuO + H_2 \rightarrow Cu_2O + H_2O$, $Cu_2O + Al_2O_3 \rightarrow 2CuAlO_2$ and/or $CuO + Al_2O_3 \rightarrow CuAl_2O_4$. $CuAlO_2$ is stable in air with the temperature range from 800 °C to 1000 °C, while $CuAl_2O_4$ is transformed into $CuAlO_2$ at the temperature of approximately 1000 °C. However, the presence of $Cu_xAl_yO_z$ phase demands a detailed characterization by using high resolution apparatus. Additionally, from micrographs of the examined samples, homogenous distribution of the present phase is clearly noticeable and the size of microstructural constituents in the range of 50–250 nm (Figure 3).

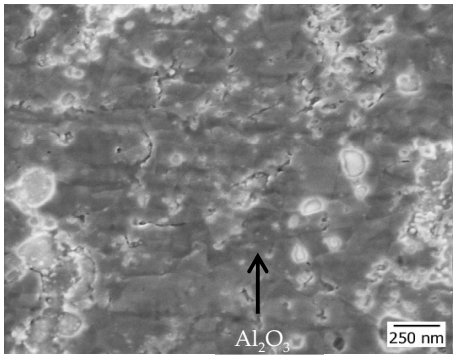

Figure 3. FIB image of compacted Cu-5wt.% Al_2O_3 composite sinter.

Additionally, the FIB analysis confirmed the analysis of structural stabilization of the system based on the values of the specific electric resistance of sintered samples ($\rho = 0.061 \times 10^{-6}$ Ω·m). Results show also that the hardness of sintered samples (HRB 10/40 (average = 124.7)) was very high for the achieved density of the sample yet lower than expected. The results of examining density, relative change of volume and the electrical and mechanical properties of sintered systems based on nanocomposite Cu-Al_2O_3 powders synthesized by the thermochemical process have been presented in previous papers by the authors [21,32].

Typical microstructure of Cu-Al_2O_3 5 wt.% is presented in Figure 4. In BF (bright field) –DF (dark field) pair, it can be seen that a copper crystal exhibits annealing twins. Twins are slightly curved, a typical feature of deformation twinning, but in the presented case, it could be a consequence of a high temperature sintering stage.

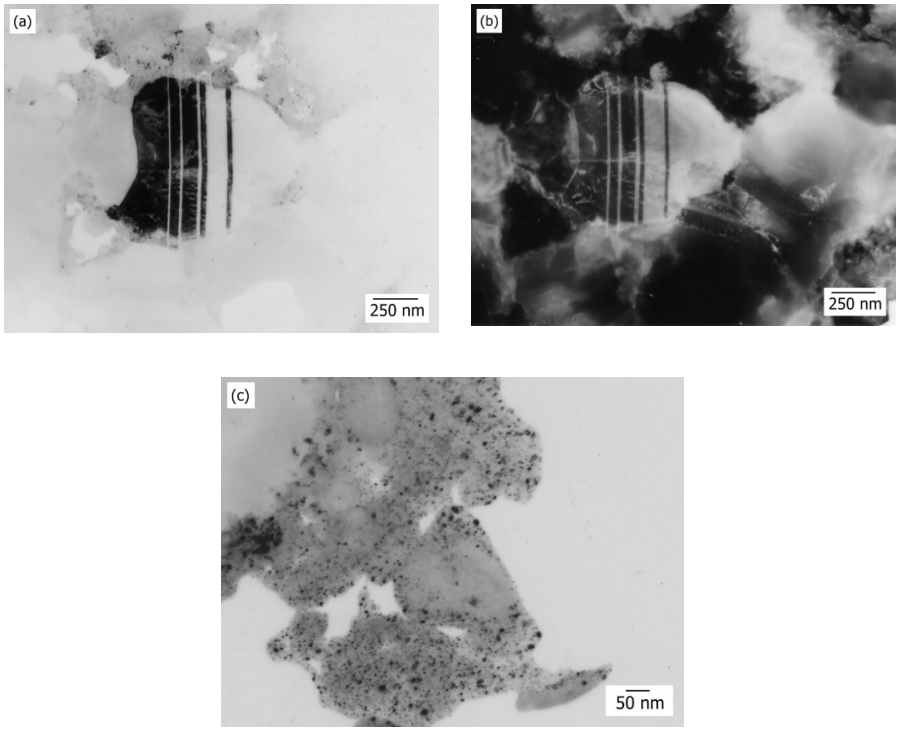

Figure 4. TEM analysis of sample after sintering: BF (bright field) and DF (dark field) images showing nano-twinning on Cu crystal (**a**,**b**), homogenous distribution of Al_2O_3 particles (**c**)

In Figure 4 a,b, a typical TEM pair bright field (BF)-centered dark field (CDF) of nanocomposite Cu-5wt.% Al_2O_3 sintered system is shown, where the well-developed crystals of copper are exposed

to twinning, despite their small size. In addition, detailed analysis indicates the detection of fine Al_2O_3 individual particles or aggregates. Conditions for twinning are accomplished when a great number of obstacles, such as homogeneously distributed Al_2O_3 particles, are created in the crystal which hamper dislocation mobility, dislocation plaits or already present twins. Since dislocations are piled up at the obstacles, in such local regions internal tension is increased, which, along with external tension, provokes creation of twins. Decreasing of dislocation mobility represents a condition for creating twin embryos; therefore, in Figure 4a,b, the clearly noticeable presence of twins indicates a decreased mobility of dislocations, i.e., stabilization of dislocation substructure, which is an elementary precondition for improving mechanical properties; i.e., reinforcing of metal materials.

Fine dark spots noticeable in the BF image (Figure 4c) present Al_2O_3 particles, size range 5–20 nm, dispersed in the copper matrix. Additionally, Figure 4c shows a homogenous distribution of Al_2O_3 particles, which is one of the requirements for dispersion of strengthened copper composites, to retain electrical conductivity of the base metal.

In a second set of TEM BF-DF pair images (Figure 5a,b) dispersion of alumina particles is also visible. Furthermore, TEM results in Figure 5a show the presence of dislocation density (the upper-right region of the grain) in a copper matrix surrounding the alumina particles, additionally increasing the strength of the material. Additionally, in Figure 5b, Moire fringes could be observed. According to [37] inside a single copper crystal, the clusters of Al_2O_3 particles could considerably alter the surrounding lattice structure, enough to prompt formation of Moire fringes.

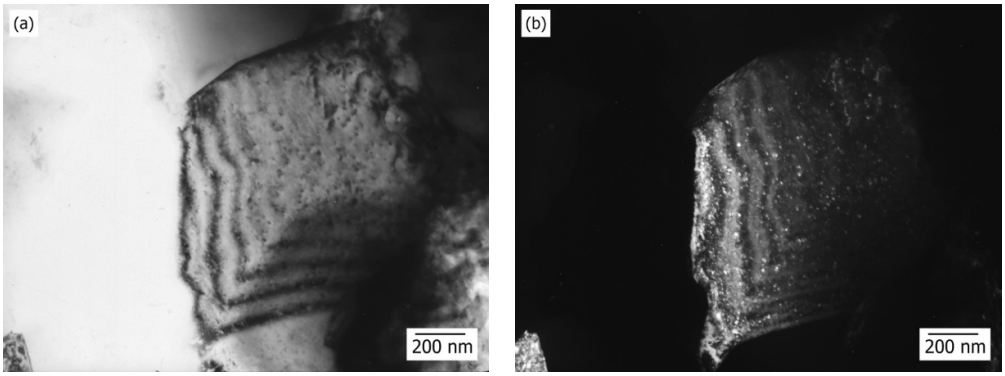

Figure 5. TEM analysis of a single copper grain containing a fine dispersion of alumina particles, dislocations and Moire fringes**.**

Figure 6a,b shows selected area diffraction patterns (SADPs), where both single spots and a Debye–Scherrer ring pattern can be observed. Single spots in SADP correspond to crystalline copper along the [111] axis, while the Debye–Scherrer rings in Figure 6b correspond to alumina Al_2O_3 particles.

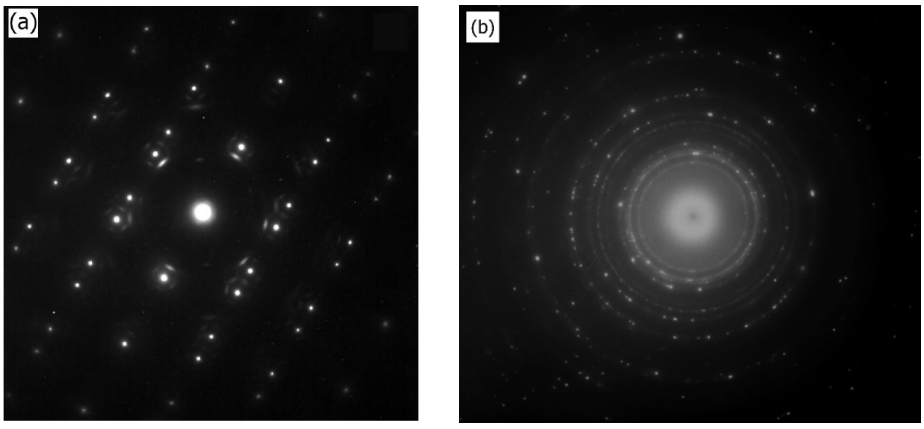

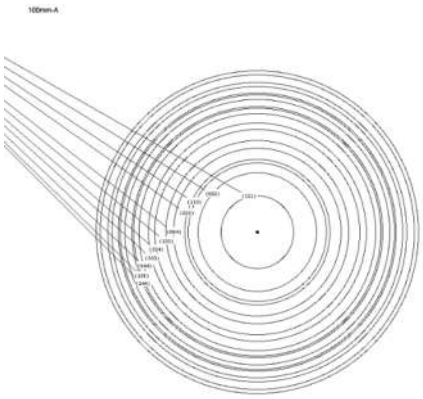

(c)

Figure 6. Selected area diffraction pattern (SADP) taken inside the grain in Figure 4: (**a**) single diffraction spots for copper along the [111] axis, (**b**) Debye–Scherrer rings for the pure Al_2O_3 particles and (**c**) inset showing the simulated Debye–Scherrer rings for γ-Al_2O_3.

In Figure 6a, besides the spots corresponding to copper, additional diffraction spots are visible, indicating presence of a solid solution. During sintering stage, formation of a third phase is possible, during eutectic reaction under suitable thermodynamic conditions at the Cu-Al_2O_3 interphase containing all three elements in a very narrow region. Existence of the third phase in the structure remains to be proven by further indexing and calculations. Composition of this phase could be, according to the literature, $CuAlO_2$ or $CuAl_2O_4$ [11,38] due to presence of an O-rich interface with larger adhesive energy [39]. Presence of this phase additionally reinforces the copper matrix by blocking the grain and sub-grain boundaries.

Ratios of measured D-values from the ring diffraction pattern are in good agreement with the calculated ratios of the corresponding g-vectors for the γ-alumina (Figure 6c).

There is a subtle difference between the crystal structure of γ-alumina and μ-alumina, yet the performed characterization via TEM did not provided a definite proof of that. It is more likely that the structure is that of γ-alumina as the original structure is boehmite and its transformation sequence does not include μ-alumina in accordance with [40].

Successful application of synthesized of the nanocomposite Cu-Al_2O_3 powders obtained by the thermochemical procedure in mechanical alloying of atomized copper powders is in detail presented in [18]. Because of high strength and electrical properties, this material can be used as electrode material for lead wires, relay blades, different contact materials and various switches, and especially for electrode materials for spot welding due to high conductivity of copper and high hardness and excellent thermal stability of aluminum.

The obtained nanocomposite powders, with structure basically preserved with the final product, provided a significant reinforcement effect in the produced sintered system. This is a consequence of homogenous distribution of the elements in the structure, accomplished during synthesis of powder and presence of the third phase which causes stabilization of dislocation substructure, accomplishing a relevant reinforcing effect and achievement of a good combination of mechanical–electric properties of the sintered systems. Comparative analyses of mechanical properties of produced composites were derived from the previous work of the authors [18–22,28,34] regarding thermo-chemical synthesis, mechanical alloying and the new synthesis method. Sintering of copper/alumina nanocomposite powders was performed at 875 °C in 60 min in laboratory electro resistant furnace in a hydrogen atmosphere in order to avoid oxidation of samples. From the presented results in Table 1, it could be concluded that use of obtained powders for mechanical alloying followed by plastic deformation have the same level of hardness with a much lower amount of Al_2O_3, which has a direct consequence through higher values of electrical conductivity. The maximal values of electrical conductivity and hardness were obtained for the sample based on 1.0 wt. % percent of Al_2O_3 in structure. Regarding

to the same chemical composition of copper/alumina nanocomposite in comparison to Amirjan [24], the values of electrical conductivity are higher in all cases, what confirms an advantage for our studied combined strategy.

Table 1. Comparison of the electrical conductivity and hardness values (HRF) after sintering at 875 °C and 60 min in our work with values of Amirjan [24].

Temperature (°C)	Time (min)	Electrical Conductivity ($MS \cdot m^{-1}$)	Electrical Conductivity, (% IACS *)		Rockvell Hardness Values (HRF)	
1.0 wt. % Al_2O_3						
875	60	33.20	57.24	55.93 [24]	50	49 [24]
1.5 wt. % Al_2O_3						
875	60	28.92	49.86	48.61 [24]	40	38 [24]
2.0 wt. % Al_2O_3						
875	60	21.95	37.84	34.80 [24]	26	25 [24]

* IACS (International Annealed Copper Standard).

After annealing at 800 °C, hardness and electrical conductivity amounted to 58 HRF and 61.78% IACS, respectively.

The proposed strengthening mechanism is presented in Figure 7. The mechanism combines the strengthening in thermo-chemically synthesized composites and strengthening during mechanical alloying.

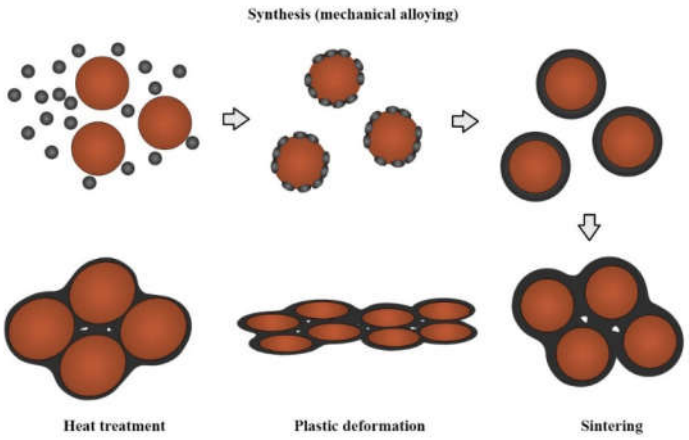

Figure 7. Microstructure transformation induced by following technological steps: mechanical alloying, heat treatment, plastic deformation and sintering.

Throughout thermo-chemical synthesis, copper base strengthening is achieved by dispersion of fine particles of Al_2O_3, and strengthening by grain boundaries, as presented in this paper. As reported by Amirjan [24] with respect to strengthening mechanism of Orawan, with increasing reinforcement amount, the distances between particles in the microstructure will decrease. Therefore, the dislocations can encompass the particles easily and lead to lower values of hardness. We assume the grain size of the composite matrixes microstructure increases with increasing sintering time. According to Hall–Petch effect, larger grain size in microstructure leads to a decrease in hardness values.

During mechanical alloying of atomized copper particles, copper-alumina composites are built into its surface. Along with the process of sintering occurs the formation of the compact structure and formation of the third phase on the grain boundary, which causes strengthening on the grain boundaries. Due to the plastic deformation, the deformation strengthening occurs, and after heat treatment, the strengthening by annealing occurs. The annealing treatment increases the system's

strength by reducing dislocation emission sources and improves material ductility through strengthening grain boundaries' resistance to intergranular cracks

4. Conclusions

Characterization of produced nanostructured composites in system Cu-Al_2O_3 showed the possibility of their synthesis via a thermochemical route. The mechanism of formation of copper-alumina nanocomposite was studied using thermodynamic analysis of drying, thermal decomposition, reduction step and homogenization. The reduction of thermally treated powders was performed in hydrogen with flow rate 20 L/h at 350 °C for one hour, where copper oxide was transformed into elementary copper, while Al_2O_3 remained unchanged.

By AEM analysis it was confirmed that homogenous distribution of Al_2O_3 particles was achieved by the thermochemical route followed by cold pressing and sintering, a necessary requirement for retaining electrical conductivity of the base metal.

Increasing of the strength of the material was achieved by presence of dislocation density in a copper matrix surrounding the alumina particles, confirmed by TEM analysis.

Additionally, the selected area diffraction pattern showed the possible presence of a third phase formed during the sintering stage at interphase containing all three elements in a very narrow region, which additionally reinforces the copper matrix by blocking the grain and sub-grain boundaries. The existence of the third phase in the structure remains to be proven by further indexing and calculations. The proposed strengthening mechanism combines the strengthening in thermo-chemically synthesized composites and strengthening during mechanical alloying. The maximal values of electrical conductivity and hardness were obtained for the sample based on 1.0 wt. % percent of Al_2O_3 in structure. Regarding the same chemical composition of copper/alumina nanocomposite in comparison to literature values by Amirjan [24], the values of electrical conductivity and hardness are higher in all cases, which confirms an advantage for our studied combined strategy.

The future study can be focused on the kinetics of the thermochemical synthesis of the studied nanocomposites. The economic size (cost effect) of this method shall be calculated via partial operations. This is a practical way for manufacturing these composites for powder metallurgy based on different applications.

Author Contributions: M.K. conceptualized and managed the research, and co-wrote the paper together with the other co-authors. Z.K. ensured financial support, supervised M.K. and co-wrote the paper. Z.A. participated in analysis and discussion of the obtained results and co-wrote this paper. S.S. helped in discussion of the results and co-wrote this paper. All authors have read and agreed to the published version of the manuscript.

Funding: This research received no external funding.

Acknowledgement: Ministry of Education, Science and Technological development of Republic of Serbia through project TR34033 financially supported the research presented within this paper.

Conflicts of Interest: The authors declare no conflict of interest.

References

1. Poole, C.P.; Owens, F.J. *Introduction to Nanotechnology*; John Wiley & Sons: Hoboken, NJ, USA, 2003.
2. Eckert, J.; Reger-Leonhard, A.; Weiß, B.; Heilmaier M. Nanostructured materials in multicomponent alloy systems. *Mater. Sci. Eng. A* **2001**, *301*, 1–11.
3. Tian, B.H.; Liu, P.; Song, K.X.; Li, Y.; Liu, Y.; Ren, F.Z.; Su, J.H. Microstructure and properties at elevated temperature of a nano-Al_2O_3 particles dispersion-strengthened copper base composite. *Mater. Sci. Eng. A* **2006**, *435–436*, 705–710.
4. Naser, J.; Ferkel, H.; Riehemann, W. Grain stabilisation of copper with nanoscaled Al_2O_3-powder. *Mater. Sci. Eng. A* **1997**, *234–236*, 470–473.

5. Trojanová, Z.; Ferkel, H.; Luká, P.; Naser, J.; Riehemann, W. Thermal stability of copper reinforced by nanoscaled and microscaled alumina particles investigated by internal friction. *Scr. Mater.* **1990**, *40*, 1063–1069.
6. Song, J.; Koch, V.; Wang, l.; Stopic, S.; Bogovic, J.; Friedrich, B.; Möbius, A.; Fuhrmann, A. Nanoscale Particles enhanced Gold Plating. *Adv. Mater. Res.* **2011**, *320*, 210–215.
7. Casati, R.; Vedani, M. Metal Matrix Composites Reinforced by Nano-Particles—A Review. *Metals* **2014**, *4*, 65–83.
8. Fathy, A.; Shehata, F.; Abdelhameed, M.; Elmahdy, M. Compressive and wear resistance of nanometric alumina reinforced copper matrix composites. *Mater. Des.* **2012**, *36*, 100–107.
9. Plascencia, G.; Utigard, T.A. High temperature oxidation mechanism of dilute copper aluminium alloys. *Corros. Sci.* **2005**, *47*, 1149–1163.
10. Lianga, S.; Fana, Z.; Xua, L.; Fangb, L. Kinetic analysis on Al_2O_3/Cu composite prepared by mechanical activation and internal oxidation. *Compos. Part A-Appl. Sci. Manuf.* **2004**, *35*, 1441–1446.
11. Jena, P.K.; Brocchi, E.A.; Solórzano, I.G.; Motta, M.S. Identification of a third phase in Cu–Al_2O_3 nanocomposites prepared by chemical routes. *Mater. Sci. Eng. A* **2004**, *371*, 72–78.
12. Brocchi, E.A.; Motta, M.S.; Solorzano, I.G.; Jena, P.K.; Moura, F.J. Alternative chemical-based synthesis routes and characterization of nano-scale particles. *Mater. Sci. Eng. B* **2004**, *112*, 200–205.
13. Lü, L.; Lai, M.O.; Zhang, S. Modeling of the mechanical-alloying process. *Mater. Process. Technol.* **1995**, *52*, 539–546.
14. Fathy, A.; Wagih, A.; El-Hamid, M.A.; Hassan, A.A. The effect of Mg add on morphology and mechanical properties of Al–*x*Mg/10Al_2O_3 nanocomposite produced by mechanical alloying. *Adv. Powder Technol.* **2014**, *25*, 1345–1350.
15. Zebarjad, S.M.; Sajjadi, S.A. Microstructure evaluation of Al–Al_2O_3 nanocomposite produced by mechanical alloying method. *Mater. Des.* **2006**, *27*, 684–688.
16. Dash, P.K.; Murty, B.S.; Karthik Aamanchi, R.B. Synthesis and Mechanical Characterisation of Aluminium-Copper-Alumina Nano Composites Powder Embedded in Glass/Epoxy Laminates. *Am. J. Nanomaterials* **2015**, *3*, 28–39.
17. Shehata, F.; Abdelhameed, M.; Fathy, A.; Elmahdy, M. Preparation and characteristics of Cu-Al_2O_3 nanocomposite. *Open. J. Metal.* **2011**, *1*, 25–35.
18. Korać, M.; Kamberović, Ž.; Anđić, Z.; Filipović, M. Nanocomposites and Polymers with Analytical Methods. In *Sintered Materials Based on Copper and Alumina Powders Synthesized by a Novel Method*; Publisher: InTech: London, UK, 2011; pp. 181–198.
19. Korać, M.; Kamberović, Ž.; Filipović, M. Determination of Al_2O_3 particle size in Cu-Al_2O_3 nanocomposite materials using UV spectrophotometry. *J. Metall. Metal.* **2008**, *14*, 279–284. (in Serbian)
20. Korać, M.; Kamberović, Ž.; Tasić, M.; Gavrilovski, M. Nanocomposite powders for new contact materials based on copper and alumina. *Chem. Ind. Chem. Eng. Q* **2008**, *14*, 215–218.
21. Anđić, Z.; Korać, M.; Kamberović, Ž.; Vujović, A.; Tasić, M. Analysis of the Properties of a Cu-Al_2O_3 Sintered System based on Ultra Fine and Nanocomposite Powders. *Sci. Sinter.* **2007**, *39*, 145–152.
22. Andić Z., Korać M., Tasić M., Raić K., Kamberović Ž., The synthesis of ultrafine and nanocomposite powders based on copper, silver and alumina, *Kovove Mater* **2006**, *44*, 145–150.
23. Seyedraoufi, Z.A.; Saghafian, H.; Shabestari, S.G. Thermochemical synthesis of nanostructured Cu-Al_2O_3 composite powder. *Chem. Ind. Chem. Eng. Q* **2014**, *20*, 339–344.
24. Amirjan, M.; Khorsand, H.; Siadati, M.H.; Farsani, R.E. Artificial Neural Network prediction of Cu–Al_2O_3 composite properties prepared by powder metallurgy method. *J. Mater. Res. Technol.* **2013**, *2*, 351–355.
25. Lara-Guevara, A.; Rojas-Rodriguez, I.; Hernandez, R.V.; Bernal-Correa, R.A.; Sierra-Gutierrez, A.; Herrera-Ramos, A.; Rodriguez-Garcia, M.E. Synthesis of copper-alumina composites by mechanical milling: An analysis. *Mater. Manuf. Processes* **2013**, *28*, 157–162.
26. Han, S.J.; Seo, J.; Choe, K.H.; Kim, M.H. Fabrication of Al_2O_3 dispersion strengthened copper alloy by spray, in-situ synthesis casting process. *Met. Mater. Int.* **2015**, *21*, 270–275.
27. Mohammadi, E.; Nasiri, H.; Khaki, V.J.; Zebarjad, S.M. Copper-alumina nanocomposite coating on copper substrate through solution combustion. *Ceram. Inter.* **2018**, *44*, 3226–3230.
28. Anđić, Z.; Korać, M.; Tasić, M.; Kamberović, Ž.; Raić, K. Synthesis and sintering of Cu-Al_2O_3 nanocomposite powders produced by a thermochemical route. *Metal. J. Metall.* **2007**, *13*, 71–82.

29. Errandonea, D. High-pressure melting curves of the transition metals Cu, Ni, Pd, and Pt. *Phys. Rev. B* **2013**, *87*, 054108.
30. Zhang, S. Melting Temperature of Al_2O_3 under Pressure. *Adv Mat Res* **2012**, *549*, 745–48.
31. Anđić, Z.; Tasić, M.; Korać, M.; Jordović, B.; Maričić, A. Influence of alumina content on the sinterability of the Cu-Al_2O_3 pseudo alloy (composite). *Mater. Technol.* **2004**, *38*, 245–248.
32. Korać, M.; Anđić, Z.; Tasić, M.; Kamberović, Ž. Sintering of Cu–Al_2O_3 nanocomposite powders produced by a thermochemical route. *J. Serb. Chem. Soc.* **2007**, *72*, 1115–1125.
33. Lee, D.W.; Ha, G.H.; Kim, B.K. Synthesis of Cu-Al_2O_3 nano composite powder. *Scr. Mater.* **2001**, *44*, 2137–2140.
34. Anđić, Z.; Vujović, A.; Tasić, M.; Korać, M.; Kamberović, Ž. Synthesis and Characterization of Dispersion Reinforced Sintered System Based on Ultra Fineand Nanocomposite Cu-Al_2O_3 Powders. In *Nanocrystal*; InTech: London, UK, 2011; pp. 217–236.
35. Entezarian, M.; Drew, R.A.L.; Direct bonding of copper to aluminum nitride. *Mater. Sci. Eng.* **1992**, *A212*, 206.
36. Jena, P.K.; Brocchi, E.A.; Motta, M.S. Characterization of Cu–Al_2O_3 nano-scale composites synthesized by in situ reduction. *Mater. Sci. Eng.* **2001**, *C15*, 175–177.
37. Tu, J.F. TEM Nano-Moiré Pattern Analysis of a Copper/Single Walled Carbon Nanotube Nanocomposite Synthesized by Laser Surface Implanting. *C* **2018**, *4*, 1–19.
38. Yi, S.; Trumble, K.P.; Gaskell, D.R. Thermodynamic analysis of aluminate stability in the eutectic bonding of copper with alumina. *Acta Mater.* **1999**, *47*, 3221–3226.
39. Tanaka, S.; Yang, R.; Kohyama, M.; Sasaki, T.; Matsunaga, K.; Ikuhara, Y. First-Principles Characterization of Atomic Structure of Al_2O_3(0001)/Cu Nano-Hetero Interface. *Mater. Trans. JIM* **2004**, *45*, 1973–1977.
40. Zhou, R.S.; Snyder, R.L. Structures and transformation mechanisms of the η, γ and θ transition aluminas. *Acta Crystallogr., Sect. B: Struct. Sci.* **1991**, *47*, 617–630.